Published in final edited form as:

Mol Cancer Res. 2018 October ; 16(10): 1523–1529. doi:10.1158/1541-7786.MCR-18-0281.

Daxx Functions are p53-independent In Vivo

Amanda R. Wasylishen[1], **Jeannelyn S. Estrella**[2], **Vinod Pant**[1], **Gilda P. Chau**[1], and **Guillermina Lozano**[1,*]

[1]Department of Genetics, The University of Texas MD Anderson Cancer Center, Houston, TX, United States of America

[2]Department of Pathology, The University of Texas MD Anderson Cancer Center, Houston, TX, United States of America

Abstract

Mutations in the death domain-associated protein (DAXX) have been recently identified in a substantial proportion of human pancreatic neuroendocrine tumors (PanNETs). Remarkably, however, little is known about the physiological role(s) of DAXX despite in vitro studies suggesting potential functions. Most prominently, and supported by tumor sequencing data, DAXX functions in concert with alpha thalassemia/mental retardation X-linked (ATRX) as a histone chaperone complex for the H3.3 variant. Studies have also identified potential roles in apoptosis, transcription, and negative regulation of the p53 tumor suppressor pathway. Herein, a mouse modeling approach was used to specifically address the latter and no significant genetic interaction between Daxx and the p53 pathway was determined. The embryonic lethal phenotype of Daxx loss is not p53-dependent. Additionally, Daxx heterozygosity does not sensitize mice to a sub-lethal dose of ionizing radiation or alter the survival or tumor phenotype of Mdm2 transgenic mice. However, the data support a tumor suppressor role for DAXX as low-dose ionizing radiation produced a higher proportion of carcinomas in Daxx heterozygous mice than wild-type controls.

Introduction

Next generation sequencing of human tumors has identified novel candidates as potential drivers of tumorigenesis. Specifically, loss of function mutations in *DAXX* were identified in over 20% of pancreatic neuroendocrine tumors (PanNETs), implicating an important tumor suppressor role for DAXX (1, 2). Given the prominence of DAXX loss in these tumors and the diversity of functions that have been attributed to Daxx *in vitro* (apoptosis, transcription, regulation of the p53 tumor suppressor pathway, and activity as a histone chaperone), a better understanding of the functions of DAXX *in vivo* is needed.

DAXX was first identified in a two-hybrid screen for novel FAS-interacting proteins, and subsequently named death domain associated protein (3). Overexpression of DAXX activates JNK signaling downstream of FAS and increases the apoptotic response of HeLa

*Corresponding author: Guillermina Lozano, The University of Texas MD Anderson Cancer Center, Department of Genetics, 1515 Holcombe Blvd, Unit 1010, Houston, TX 77030, gglozano@mdanderson.org, Phone: 713-834-6386, Fax: 713-834-6380.

Conflict of interest:
The authors declare no potential conflicts of interest.

and 293 cells. Opposing this pro-apoptotic function, DAXX has also been characterized as a negative regulator of the p53 tumor suppressor pathway. There are two reported mechanisms of regulation. First, DAXX directly binds the C-terminal domain of p53 and inhibits transactivation of p53 targets and downstream induction of cell death (4). Additionally, DAXX forms a complex with MDM2, the E3 ubiquitin ligase that targets p53 for degradation, and the deubiquitylating enzyme HAUSP. Interaction with HAUSP mediates the deubiquitylation and subsequent stabilization of MDM2, allowing for efficient attenuation of p53 activity (5). Consistent with functioning as a negative regulator of the p53 pathway, *Daxx* knockout mice are post-implantation lethal and demonstrate a robust induction of apoptosis, as measured by terminal deoxynucleotidyl transferase dUTP nick end labeling (TUNEL) (6). Embryonic stem cells isolated from blastocysts also show an increase in sub-G1 fraction and an increase in DNA laddering. Combined these data support an anti-apoptotic function of Daxx in development.

DAXX also has established roles as an epigenetic regulator. DAXX and ATRX were first found to interact through immunoprecipitation of Hela cell extracts, and shown to colocalize to PML nuclear bodies (7). Subsequent studies have demonstrated that DAXX and ATRX function as chaperones for the histone variant H3.3, and specifically incorporate H3.3 into heterochromatic DNA regions including telomeres (8, 9). The mutual exclusivity of *DAXX* and *ATRX* mutations in PanNETs suggests this shared function is required for tumor suppression (1). *DAXX* and *ATRX* mutations also associate with activation of the alternative lengthening of telomeres pathway, suggesting that the incorporation of H3.3 is important for telomere maintenance (10).

In this study, we use a *Daxx*-null allele to examine its role in regulating the p53 tumor suppressor pathway *in vivo*. While we identify no significant regulation of the p53 tumor suppressor pathway in the mouse, we present data to support Daxx as tumor suppressor, as there is a significant increase in the proportion of mice that develop carcinomas in heterozygous mice treated with a low dose of radiation compared to wild-type controls.

Materials and Methods

Mice and tumor analysis

All mouse experiments were performed in compliance with the MD Anderson Cancer Center Institutional Animal Care and Use Committee. $Daxx^{tm2Led}$ mice (JAX Stock #008669) and p53-null mice (JAX Stock #002101) were obtained from The Jackson Laboratory (Bar Harbor, ME, USA). *Zp3-Cre* (JAX Stock #0036510) and CMV-CreTg (11) mice were obtained from The University of Texas MD Anderson Genetically Engineered Mouse Facility. $Mdm2^{Tg}$ (NCI mouse repository stock #01XJC) and $Mdm2^{P2/P2}$ mice have been previously described (12, 13). Primers used for *Daxx* genotyping, as indicated in Figure 1, are F: 5’-AGCAGTAACTCCGGTAGTAGGAAG-3’, R1: 5’-AGGAACGGAACCACCTCAG-3’, and R2: 5’-GAAGGCGGCGAGCCAATGTG-3’. Mice were maintained on a mixed C57BL/6 and 129S6/SvEvTac background, and all experiments were conducted with littermate controls. Mice were sacrificed upon morbidity or after reaching the 2-year endpoint of the study.

Radiation

To evaluate radiosensitivity, six- to eight-week old mice were irradiated with 6 Gy in a Cesium-137 irradiator and monitored for survival for 30 days. To evaluate radiation-induced tumorigenesis, four-week old mice were treated with 4 weekly doses of 0.7 Gy ionizing radiation and monitored for tumorigenesis for up to 2 years.

Histology and immunohistochemistry

Collected tissues were fixed in 10% formalin and paraffin embedded for sectioning. Sections were dewaxed and rehydrated according to standard protocols and stained with hematoxylin and eosin (H&E). Cytokeratin immunohistochemistry was performed using standard methods with citrate buffer for antigen retrieval and stained with anti-wide spectrum cytokeratin antibody (Abcam #ab9377). Antigen retrieval for Chromogranin A (Abcam # ab45179) and synaptophysin (Abcam #ab32127) immunohistochemistry was performed using Tris/EDTA buffer pH 9. Visualization was performed using ABC and DAB kits (Vector Laboratories) and slides were counterstained with hematoxylin.

Western blotting

Tissue samples were flash frozen, pulverized, and lysed in SDS lysis buffer (1% SDS, 6.5 mM TRIS-HCl pH=6.8, 25% glycerol, 10% β-mercaptoethanol). Protein extracts were separated by SDS-PAGE, transferred to nitrocellulose membranes, and probed with antibodies against Daxx (Santa Cruz #M-112) and Vinculin (Sigma #V9131). Proteins were visualized using Li-COR secondary antibodies and scanned on a Li-COR Odyssey Imager. Quantification of scanned blots was performed using ImageJ software (NIH).

Statistical Analysis

All statistical analyses were performed using GraphPad Prism 6 software, and p-value of <0.05 was considered statistically significant. The difference between observed and expected frequencies of pups was determined by chi-squared (X^2) test. The difference between survival curves was determined using the log-rank (Mantel-Cox) test. Differences between observed and expected tumor spectra were determined by chi-squared (X^2) test using the proportions from controls as the expected values.

Results

We obtained the available conditional *Daxx* allele ($Daxx^{tm2Led}$) from The Jackson Laboratories (Figure 1A). To generate a germline null allele for our studies, we crossed $Daxx^{tm2Led}$ to a *CMV-Cre* mice and were surprised to find little or no evidence of recombination of the targeted locus in progeny at weaning. We subsequently sequenced the locus and identified a single nucleotide deletion in the proximal loxP site contained within intron 2 (Figure 1B), which rendered recombination inefficient *in vivo*. Despite this mutation, we were able to obtain a germline $Daxx^{\Delta 3}$ allele by crossing with the stronger *Zp3-Cre* deleter mouse (Figure 1C). Thus, while inefficient, recombination is possible with the mutant loxP site, consistent with a previous publication that showed some recombination using a lentiviral Cre recombinase *ex vivo* (14). However, these results generally suggest that this allele will only have limited utility *in vivo*.

This new *Daxx*$^{\Delta 3}$ allele is different than the previously published *Daxx*-null allele which replaced a 2.5 kb region containing exon 2 and most of exon 3 with a neomycin resistance cassette (6). The deletion of exon 3 results in a frame shift of 22 amino acids and a premature stop. We first evaluated the expression of Daxx protein in tissues from 6 week old mice. Western blot analysis reveals a decrease in Daxx protein in all tissues assayed (pancreas, liver and spleen) from Daxx heterozygous mice compared to wild-type controls (Figure 1D). We next evaluated the phenotype of homozygous *Daxx*$^{\Delta 3/\Delta 3}$ mice. We intercrossed *Daxx*$^{\Delta 3/+}$ mice and genotyped pups at weaning and identified no *Daxx*$^{\Delta 3/\Delta 3}$ animals, confirming the previously reported *Daxx*-null embryonic lethality (6). Timed pregnancies indicated that null embryos were phenotypically distinct as early as E8.5 and clearly different at E9.5 (Figure 1E), as previously reported for a different null allele.

The early lethality of the first *Daxx*-null mouse was previously reported to be accompanied by an increase in apoptosis, suggesting that Daxx may have anti-apoptotic roles in development (6). Additionally, data suggest that DAXX is a negative regulator of the p53 pathway *in vitro* (15), implicating increased p53 activity as the cause of lethality, similar to *Mdm2*-null mice (16–18). If Daxx is an important negative regulator of the p53 pathway during development, we hypothesized that *Daxx*-null embryonic lethality would be rescued by concomitant loss of *p53*. We intercrossed *Daxx*$^{\Delta 3/+}$*p53*$^{+/-}$ mice and evaluated genotypes of progeny at weaning. *p53* loss was unable to rescue the *Daxx*-null lethality as no *Daxx*$^{\Delta 3/\Delta 3}$*p53*$^{-/-}$ animals were identified at weaning (Table 1, X^2 **** p<0.0001). We further evaluated if *p53* loss was able to prolong the development of *Daxx*-null embryos. Timed matings of *Daxx*$^{\Delta 3/+}$*p53*$^{+/-}$ females and *Daxx*$^{\Delta 3/+}$*p53*$^{-/-}$ males were set up and embryos dissected at E9.5. We evaluated 32 embryos from 8 litters and identified 4 *Daxx*$^{\Delta 3/\Delta 3}$*p53*$^{-/-}$ embryos, all indistinguishable from *Daxx*$^{\Delta 3/\Delta 3}$ embryos (Figure 1E), indicating that p53 loss is unable to prolong the development of *Daxx*-null mice.

To next evaluate the effect of Daxx as a regulator of the p53 pathway in the adult mouse, we assayed the response of heterozygous animals to a sub-lethal dose of radiation. *Mdm2*$^{+/-}$ mice are radiosensitive and do not survive a single sublethal dose of ionizing radiation (IR) due to p53-dependent bone marrow aplasia (13, 19). Similarly, mice with a defective p53-Mdm2 feedback loop (*Mdm2*$^{P2/P2}$) have an elevated p53 response and are sensitive to the same sublethal dose of IR (13). If Daxx also negatively regulates the p53 pathway, we hypothesized that *Daxx*$^{\Delta 3/+}$ mice would be similarly radiosensitive. Wild-type, *Daxx*$^{\Delta 3/+}$ and *Mdm2*$^{P2/P2}$ mice were treated with 6 Gy IR and followed for 30 days post-treatment (Figure 2A), as bone marrow toxicity is usually observed in the first few weeks following treatment. As expected, *Mdm2*$^{P2/P2}$ control mice were radiosensitive, but no toxicity was observed in either wild-type or *Daxx*$^{\Delta 3/+}$ genotype, suggesting that Daxx is not a potent regulator of Mdm2 or the p53 pathway in response to IR *in vivo* (Figure 2B).

To investigate genetic interaction between Daxx and the p53 pathway in a pathogenic context, we evaluated whether *Daxx* heterozygosity would impact *Mdm2* overexpression-induced tumorigenesis. Specifically, if Daxx negatively regulates the p53 pathway through stabilization of Mdm2, we predicted Daxx loss would delay Mdm2-induced tumorigenesis. Transgenic expression of *Mdm2* is sufficient to promote tumorigenesis in mice (12). We therefore established a cohort of *Mdm2*^{Tg} and *Mdm2*^{Tg}*Daxx* $^{\Delta 3/+}$ littermates and followed it

for tumorigenesis for 2 years. Mice were on a mixed (C57BL/6 and 129S6/SvEvTac) background. There was no significant difference in survival between these groups (Figure 2C), with median survivals of 663 and 665 days, respectively. We additionally noted no remarkable difference in tumor spectrum between these two groups (Figure 2D, Table 2), with the majority of mice developing lymphomas, with some sarcomas, and an occasional carcinoma (hepatocellular carcinoma). *Daxx*$^{\Delta 3/+}$ control mice were generally healthy and tumor free throughout the course of this study, with no significant morbidity.

As mutations in the DAXX/ATRX/H3.3 axis have now been identified in several different tumor types, including PanNETs, glioblastomas, giant cell tumors of the bone and chondroblastomas (1, 20–22), we next evaluated the potential tumor suppressor activity in *Daxx* heterozygous mice in cooperation with low dose IR. IR induces DNA double-strand breaks which introduce mutations that can provide additional cooperating events required for efficient tumorigenesis. Mice were treated with four weekly doses of 0.7Gy IR starting at 4 weeks of age (Figure 3A). This dosing strategy has been used in the past to sensitize mice to tumorigenesis (23, 24). Mice were monitored until moribund or for 2 years. There was no significant difference in survival of *Daxx*$^{\Delta 3/+}$ compared to wild-type controls, with mean survivals of 718 and 721 days, respectively (Figure 3B). We evaluated the tumor spectrum of moribund or autopsied mice and identified a significant increase in the proportion of carcinomas that formed in *Daxx* heterozygous mice (*p=0.013, Figure 3C, Table 3). Specifically we identified ovarian carcinomas in mice of both genotypes, and ovarian cysts in 3 of the *Daxx*$^{\Delta 3/+}$ mice (Figure 3D). Lung carcinomas were also identified in both genotypes. Finally, nasolacrimal carcinomas exclusive to *Daxx* heterozygous animals (Figure 3E). Notably, a number of mice presented with more than one tumor at necropsy, as indicated in Table 3 where the number of tumors is greater than the number of mice. In most cases, this reflected a lymphoma in addition to a sarcoma or a carcinoma. We conducted immunoblot analysis of four tumors (two lung carcinomas, and one each hepatocellular carcinoma and lymphoma) from Daxx heterozygous mice to evaluate possible loss of heterozygosity. Daxx protein is detected in all tumors, suggesting that Daxx may be functioning as a haploinsufficient tumor suppressor in response to IR (Figure 3F).

The most striking and unifying histological feature of the carcinomas was the presence of papillary architecture. The papillary carcinomas in the ovary (n=1), lung (n=8, both genotypes) and nasolacrimal ducts (n=4) show proliferation of epithelial cells (confirmed by wide spectrum cytokeratin immunohistochemical stain, Supplementary Figure 1A) lining papillae which often project into cystic spaces but are tightly packed, form anastomosing ribbons, and appear solid in areas. In the papillary areas, the epithelial cells are cuboidal to columnar with relatively uniform nuclei, indistinct nucleoli and abundant eosinophilic cytoplasm, consistent with well-differentiated papillary adenocarcinoma (Figure 3E).

As spontaneous models of ovarian carcinoma are fairly limited, we were prompted to complete necropsies on all mice at the 2-year end point of our study and identified carcinomas in an additional 4 mice (both genotypes). In total 7/22 (32%) of the female mice in this study developed ovarian carcinomas, suggesting that this low dose treatment regimen in a mixed (C57BL/6 and 129S6/SvEvTac) background might be a useful model for ovarian cancer studies.

Due to the strong association between *DAXX* mutations and PanNETs, we also conducted histopathological examination of the pancreas from all mice in this study. We identified 2 heterozygous mice with histopathologic alterations in the pancreas. One had evidence of chronic, predominantly lymphocytic inflammation and a hyperplasia characterized by proliferation of islet cells (small, centrally located, cytologically bland nuclei with coarsely clumped chromatin and moderate amphophilic cytoplasm) forming confluent nests (Figure 3G, left panel). A second had a well-differentiated neuroendocrine tumor with proliferation of neuroendocrine cells (confirmed by chromogranin A, Supplementary Figure 1B, and synaptophysin immunohistochemical stains) with round to oval nuclei (slightly larger than adjacent islet cell nuclei), coarsely clumped chromatin and amphophilic cytoplasm. The neuroendocrine cells show trabecular architecture surrounded by small vessels and minimal fibrotic stroma (Figure 3G, right panel).

Discussion

The physiologically relevant functions of DAXX remain controversial. There are *in vitro* data supporting both pro- and anti-apoptotic roles in the cell, as well as functions in transcriptional activation and repression, chromatin maintenance through histone chaperone activity, and regulation of the p53 tumor suppressor pathway. Herein, we have used mouse models to specifically interrogate the potential genetic interaction between Daxx and the p53 pathway *in vivo*. While *Daxx*-null mice exhibit early lethality and induction of apoptosis, key characteristics of mice deficient for p53 negative regulators *Mdm2* and *Mdm4*, *Daxx*-null mice could not be similarly rescued on a *p53*-null background (16, 17, 25). These data suggest that the apoptosis induced in the *Daxx*-null embryo is not a direct result of p53 induction. Rather, apoptosis is likely an indirect consequence of the loss of some other function of Daxx. For example, the lethality may be driven by genomic instability due to the loss of H3.3 chaperone activity. Consistent with this, the conditional deletion of *Atrx* using tissue specific Cre-recombinase lines generally leads to DNA damage, p53 pathway activation and cell death *in vivo* (26–30); however, while the extent of cell death is reduced in a p53-deficient background, the phenotype is not rescued and there is an enhanced accumulation of DNA damage (26). Further, if Daxx is a positive regulator of Mdm2 stability, we predicted *Daxx* heterozygosity would delay tumorigenesis driven by the $Mdm2^{Tg}$. Both the survival and tumor spectrum of $Mdm2^{Tg}$ mice were not altered in a *Daxx* heterozygous background. Combined these data suggest that there is no physiologically relevant genetic interaction between Daxx and the p53 pathway *in vivo*.

Similar results have been obtained when other candidate regulators of the p53 pathway have been studied in mice. For example, Diexf was identified as a negative regulator of p53 in zebrafish, but studies in the mouse similarly demonstrate that *p53* loss is unable to rescue the early lethality of *Diexf*-null embryos, and heterozygous animals showed no evidence of enhanced radiosensitivity (31). Cell culture studies identified Pirh2 as both a p53-transcriptional target and an E3 ubiquitin ligase for p53 (similar to MDM2), but *Pirh2*-knockout mice are both viable and tumor prone, suggesting that p53 is not the primary physiological target of this enzyme (32, 33). Similar data are available for other regulators, including Cop1, Arfbp1 and Trim24 (34). Further, human tumor sequencing does not support a pathogenic role for DAXX in regulating the p53 pathway. Amplification of *MDM2*

and *MDM4*, genes that encode two essential negative regulators of p53, occur in several tumor types and are mutually exclusive with p53 mutations (35). Cancer genome data available through the cBio portal (36, 37), demonstrates that the most frequent alterations in *DAXX* occur in PanNETs, and these are loss of function alleles.

To date, the most compelling data to identify a physiological role for DAXX *in vivo* is the sequencing data from human PanNETs. *DAXX* mutations are mutually exclusive with *ATRX* mutations, strongly suggesting that it is the loss of their shared function as a H3.3 chaperone complex that is contributing to tumorigenesis, and proper H3.3 incorporation is essential for homeostasis in the endocrine pancreas. While recurrent *DAXX* mutations have only been identified in PanNETs, mutations in *ATRX* and the genes that code for H3.3 (*H3F3A* and *H3F3B*) have been identified in additional tumor types suggesting that alterations in this axis contribute more broadly to tumorigenesis (20, 21). As dysregulation of genes and pathways can occur through mechanisms independent of direct DNA mutations and to take an unbiased approach to study the potential role for Daxx as a tumor suppressor *in vivo*, we exposed a small cohort of *Daxx* heterozygous mice and wild-type controls to low dose ionizing radiation. While there was no significant difference in survival compared to controls, *Daxx* heterozygous mice did demonstrate a significant increase in the proportion of carcinomas, prominently developing nasolacrimal, ovarian and lung carcinomas, often with papillary architecture. These findings suggest that there may be other cell types sensitive to *Daxx* loss. Like PanNETs, nasolacrimal tumors are rare, and it will be interesting to evaluate tumor sequencing data if and when it becomes available for *DAXX* mutations. Although our cohort was small, we also identified early lesions, one hyperplasia and a one well-differentiated neuroendocrine tumor, in the pancreas of two *Daxx* heterozygous animals in this cohort. As the most significant pathology in Daxx heterozygous mice was observed in cooperation with a low dose of IR and given the established role of Daxx in regulating chromatin structure as a histone chaperone, it is tempting to speculate that this cooperation may be a result of increased chromosomal instability or telomere dysfunction due to Daxx heterozygosity. Taken together, results from this cohort support a tumor suppressor role for Daxx *in vivo*.

One other notable observation from this work is the high proportion of radiation-induced ovarian pathology that was identified in both genotypes, specifically ovarian carcinomas were identified in 32% of the female mice in this study. We have irradiated and followed several other cohorts of mice on different genetic backgrounds (C57BL/6 and BALB/c) and have not previously identified ovarian carcinomas (24, 38), suggesting that the 129S6/SvEvTac background may increase susceptibility to these cancers. Additionally, this is a spontaneous radiation-induced model that does not require the use of a cell-type specific Cre recombinase, and therefore circumvents concerns about targeting the correct cell of origin. Thus, this may be a useful model for future studies of ovarian tumorigenesis.

In conclusion, we have effectively used *Daxx* germline heterozygosity to evaluate Daxx as a regulator of the p53 pathway, and more generally to study the potential role for Daxx as a tumor suppressor. Future studies in which homozygous deletion of *Daxx* can be achieved both in a tissue and time-dependent manner are likely to uncover the physiologically relevant function(s) of Daxx *in vivo.*

Supplementary Material

Refer to Web version on PubMed Central for supplementary material.

Acknowledgments

We thank Dr. Stephen Jones for the *Mdm2*^{Tg} mice. This research was supported by a grants from the Neuroendocrine Tumor Research Foundation and NIH (CA47296) to G. Lozano and a fellowship from the Canadian Institutes of Health Research to A. Wasylishen. A. Wasylishen is the recipient of a Dodie P. Hawn Award in Genetics.

References

1. Jiao Y, Shi C, Edil BH, de Wilde RF, Klimstra DS, Maitra A, et al. DAXX/ATRX, MEN1, and mTOR pathway genes are frequently altered in pancreatic neuroendocrine tumors. Science. 2011;331(6021):1199–203. [PubMed: 21252315]
2. Scarpa A, Chang DK, Nones K, Corbo V, Patch AM, Bailey P, et al. Whole-genome landscape of pancreatic neuroendocrine tumours. Nature. 2017;543(7643):65–71. [PubMed: 28199314]
3. Yang X, Khosravi-Far R, Chang HY, Baltimore D. Daxx, a novel Fas-binding protein that activates JNK and apoptosis. Cell. 1997;89(7):1067–76. [PubMed: 9215629]
4. Zhao LY, Liu J, Sidhu GS, Niu Y, Liu Y, Wang R, et al. Negative regulation of p53 functions by Daxx and the involvement of MDM2. J Biol Chem. 2004;279(48):50566–79. [PubMed: 15364927]
5. Ronai Z Balancing Mdm2 - a Daxx-HAUSP matter. Nature cell biology. 2006;8(8):790–1. [PubMed: 16880812]
6. Michaelson JS, Bader D, Kuo F, Kozak C, Leder P. Loss of Daxx, a promiscuously interacting protein, results in extensive apoptosis in early mouse development. Genes & development. 1999;13(15):1918–23. [PubMed: 10444590]
7. Xue Y, Gibbons R, Yan Z, Yang D, McDowell TL, Sechi S, et al. The ATRX syndrome protein forms a chromatin-remodeling complex with Daxx and localizes in promyelocytic leukemia nuclear bodies. Proceedings of the National Academy of Sciences of the United States of America. 2003;100(19):10635–40. [PubMed: 12953102]
8. Goldberg AD, Banaszynski LA, Noh KM, Lewis PW, Elsaesser SJ, Stadler S, et al. Distinct factors control histone variant H3.3 localization at specific genomic regions. Cell. 2010;140(5):678–91. [PubMed: 20211137]
9. Lewis PW, Elsaesser SJ, Noh KM, Stadler SC, Allis CD. Daxx is an H3.3-specific histone chaperone and cooperates with ATRX in replication-independent chromatin assembly at telomeres. Proceedings of the National Academy of Sciences of the United States of America. 2010;107(32): 14075–80. [PubMed: 20651253]
10. Heaphy CM, de Wilde RF, Jiao Y, Klein AP, Edil BH, Shi C, et al. Altered telomeres in tumors with ATRX and DAXX mutations. Science. 2011;333(6041):425. [PubMed: 21719641]
11. Zinyk DL, Mercer EH, Harris E, Anderson DJ, Joyner AL. Fate mapping of the mouse midbrain-hindbrain constriction using a site-specific recombination system. Curr Biol. 1998;8(11):665–8. [PubMed: 9635195]
12. Jones SN, Hancock AR, Vogel H, Donehower LA, Bradley A. Overexpression of Mdm2 in mice reveals a p53-independent role for Mdm2 in tumorigenesis. Proceedings of the National Academy of Sciences of the United States of America. 1998;95(26):15608–12. [PubMed: 9861017]
13. Pant V, Xiong S, Jackson JG, Post SM, Abbas HA, Quintas-Cardama A, et al. The p53-Mdm2 feedback loop protects against DNA damage by inhibiting p53 activity but is dispensable for p53 stability, development, and longevity. Genes & development. 2013;27(17):1857–67. [PubMed: 23973961]
14. Michod D, Bartesaghi S, Khelifi A, Bellodi C, Berliocchi L, Nicotera P, et al. Calcium-dependent dephosphorylation of the histone chaperone DAXX regulates H3.3 loading and transcription upon neuronal activation. Neuron. 2012;74(1):122–35. [PubMed: 22500635]

15. Tang J, Qu LK, Zhang J, Wang W, Michaelson JS, Degenhardt YY, et al. Critical role for Daxx in regulating Mdm2. Nature cell biology. 2006;8(8):855–62. [PubMed: 16845383]
16. Jones SN, Roe AE, Donehower LA, Bradley A. Rescue of embryonic lethality in Mdm2-deficient mice by absence of p53. Nature. 1995;378(6553):206–8. [PubMed: 7477327]
17. Montes de Oca Luna R, Wagner DS, Lozano G. Rescue of early embryonic lethality in mdm2-deficient mice by deletion of p53. Nature. 1995;378(6553):203–6. [PubMed: 7477326]
18. Chavez-Reyes A, Parant JM, Amelse LL, de Oca Luna RM, Korsmeyer SJ, Lozano G. Switching mechanisms of cell death in mdm2- and mdm4-null mice by deletion of p53 downstream targets. Cancer research. 2003;63(24):8664–9. [PubMed: 14695178]
19. Terzian T, Wang Y, Van Pelt CS, Box NF, Travis EL, Lozano G. Haploinsufficiency of Mdm2 and Mdm4 in tumorigenesis and development. Mol Cell Biol. 2007;27(15):5479–85. [PubMed: 17526734]
20. Behjati S, Tarpey PS, Presneau N, Scheipl S, Pillay N, Van Loo P, et al. Distinct H3F3A and H3F3B driver mutations define chondroblastoma and giant cell tumor of bone. Nat Genet. 2013;45(12):1479–82. [PubMed: 24162739]
21. Schwartzentruber J, Korshunov A, Liu XY, Jones DT, Pfaff E, Jacob K, et al. Driver mutations in histone H3.3 and chromatin remodelling genes in paediatric glioblastoma. Nature. 2012;482(7384):226–31. [PubMed: 22286061]
22. Chen X, Bahrami A, Pappo A, Easton J, Dalton J, Hedlund E, et al. Recurrent somatic structural variations contribute to tumorigenesis in pediatric osteosarcoma. Cell Rep. 2014;7(1):104–12. [PubMed: 24703847]
23. Mori N, Yamate J, Umesako S, Hong DP, Okumoto M, Nakao R. Preferential induction of mammary tumors in p53 hemizygous BALB/c mice by fractionated irradiation of a sub-lethal dose of X-rays. J Radiat Res. 2003;44(3):249–54. [PubMed: 14646229]
24. Xiong S, Tu H, Kollareddy M, Pant V, Li Q, Zhang Y, et al. Pla2g16 phospholipase mediates gain-of-function activities of mutant p53. Proceedings of the National Academy of Sciences of the United States of America. 2014;111(30):11145–50. [PubMed: 25024203]
25. Parant J, Chavez-Reyes A, Little NA, Yan W, Reinke V, Jochemsen AG, et al. Rescue of embryonic lethality in Mdm4-null mice by loss of Trp53 suggests a nonoverlapping pathway with MDM2 to regulate p53. Nat Genet. 2001;29(1):92–5. [PubMed: 11528400]
26. Seah C, Levy MA, Jiang Y, Mokhtarzada S, Higgs DR, Gibbons RJ, et al. Neuronal death resulting from targeted disruption of the Snf2 protein ATRX is mediated by p53. J Neurosci. 2008;28(47):12570–80. [PubMed: 19020049]
27. Berube NG, Mangelsdorf M, Jagla M, Vanderluit J, Garrick D, Gibbons RJ, et al. The chromatin-remodeling protein ATRX is critical for neuronal survival during corticogenesis. J Clin Invest. 2005;115(2):258–67. [PubMed: 15668733]
28. Bagheri-Fam S, Argentaro A, Svingen T, Combes AN, Sinclair AH, Koopman P, et al. Defective survival of proliferating Sertoli cells and androgen receptor function in a mouse model of the ATR-X syndrome. Hum Mol Genet. 2011;20(11):2213–24. [PubMed: 21427128]
29. Huh MS, Price O'Dea T, Ouazia D, McKay BC, Parise G, Parks RJ, et al. Compromised genomic integrity impedes muscle growth after Atrx inactivation. J Clin Invest. 2012;122(12):4412–23. [PubMed: 23114596]
30. Solomon LA, Russell BA, Watson LA, Beier F, Berube NG. Targeted loss of the ATR-X syndrome protein in the limb mesenchyme of mice causes brachydactyly. Hum Mol Genet. 2013;22(24):5015–25. [PubMed: 23892236]
31. Aryal NK, Wasylishen AR, Pant V, Riley-Croce M, Lozano G. Loss of digestive organ expansion factor (Diexf) reveals an essential role during murine embryonic development that is independent of p53. Oncotarget. 2017;8(61):103996–4006. [PubMed: 29262616]
32. Leng RP, Lin Y, Ma W, Wu H, Lemmers B, Chung S, et al. Pirh2, a p53-induced ubiquitin-protein ligase, promotes p53 degradation. Cell. 2003;112(6):779–91. [PubMed: 12654245]
33. Hakem A, Bohgaki M, Lemmers B, Tai E, Salmena L, Matysiak-Zablocki E, et al. Role of Pirh2 in mediating the regulation of p53 and c-Myc. PLoS Genet. 2011;7(11):e1002360. [PubMed: 22125490]

34. Pant V, Lozano G. Limiting the power of p53 through the ubiquitin proteasome pathway. Genes & development. 2014;28(16):1739–51. [PubMed: 25128494]

35. Wasylishen AR, Lozano G. Attenuating the p53 Pathway in Human Cancers: Many Means to the Same End. Cold Spring Harb Perspect Med. 2016;6(8).

36. Cerami E, Gao J, Dogrusoz U, Gross BE, Sumer SO, Aksoy BA, et al. The cBio cancer genomics portal: an open platform for exploring multidimensional cancer genomics data. Cancer Discov. 2012;2(5):401–4. [PubMed: 22588877]

37. Gao J, Aksoy BA, Dogrusoz U, Dresdner G, Gross B, Sumer SO, et al. Integrative analysis of complex cancer genomics and clinical profiles using the cBioPortal. Sci Signal. 2013;6(269):pl1. [PubMed: 23550210]

38. Ortiz GJ, Li Y, Post SM, Pant V, Xiong S, Larsson CA, et al. Contrasting effects of an Mdm2 functional polymorphism on tumor phenotypes. Oncogene. 2018;37(3):332–40. [PubMed: 28925402]

Implications:

While DAXX has important in vivo functions, they are independent of an inhibitory role on the p53 tumor suppressor pathway.

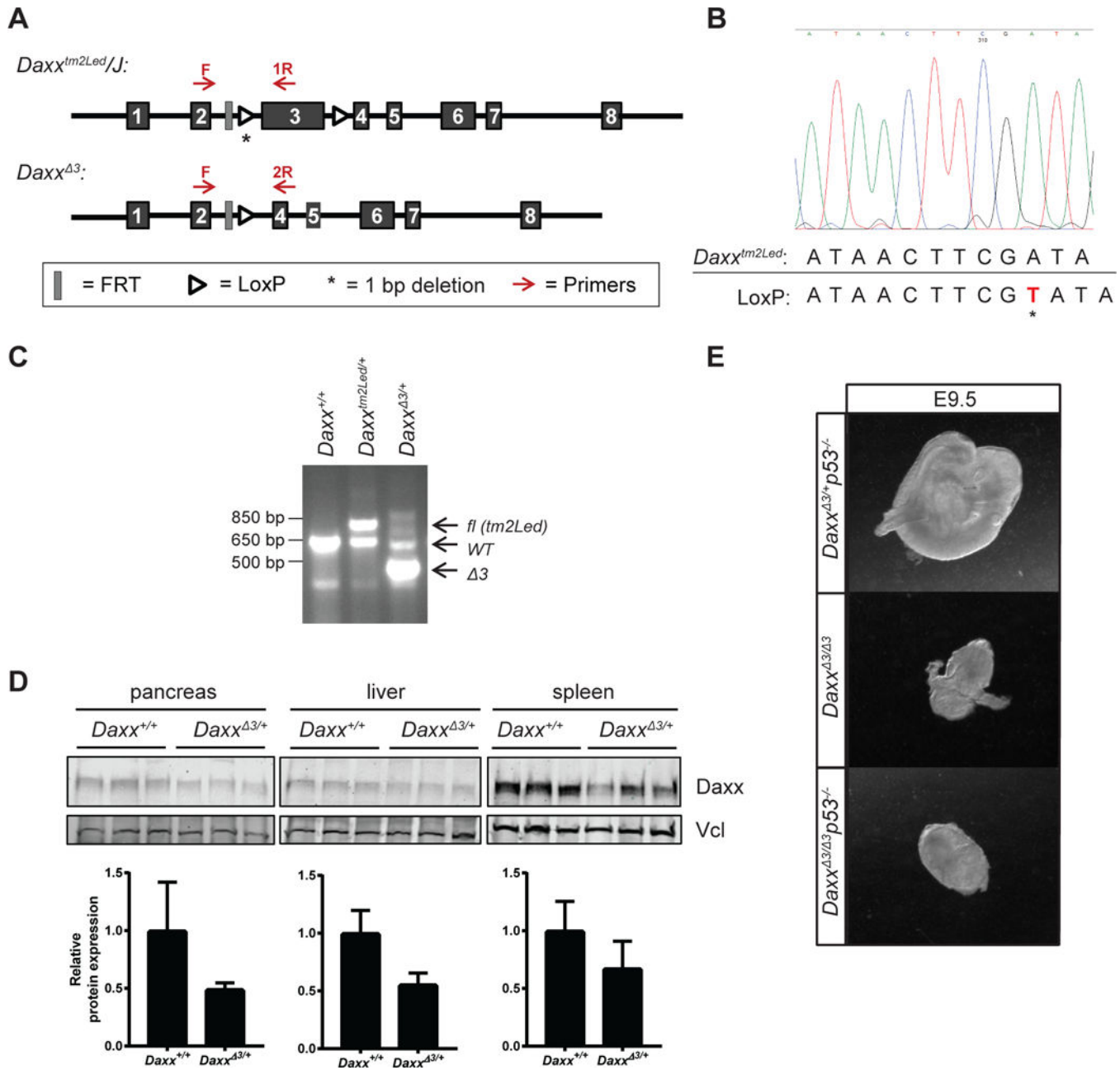

Figure 1: Generation and characterization of *Daxx*$^{\Delta 3/\Delta 3}$ mice.

A) Schematic representation of *Daxx*^{tm2Led} and *Daxx*$^{\Delta 3}$ alleles. Genotyping primers are indicated in red. B) Sanger sequencing of the intron 2 loxP site of the *Daxx*^{tm2Led} allele. C) PCR genotyping of wild-type (WT), *Daxx*^{tm2Led} and *Daxx*$^{\Delta 3}$ alleles. D) Western blot analysis of various tissues from three independent *Daxx*$^{+/+}$ and *Daxx*$^{\Delta 3/+}$ mice. Vcl, vinculin. E) Representative images of E9.5 embryos.

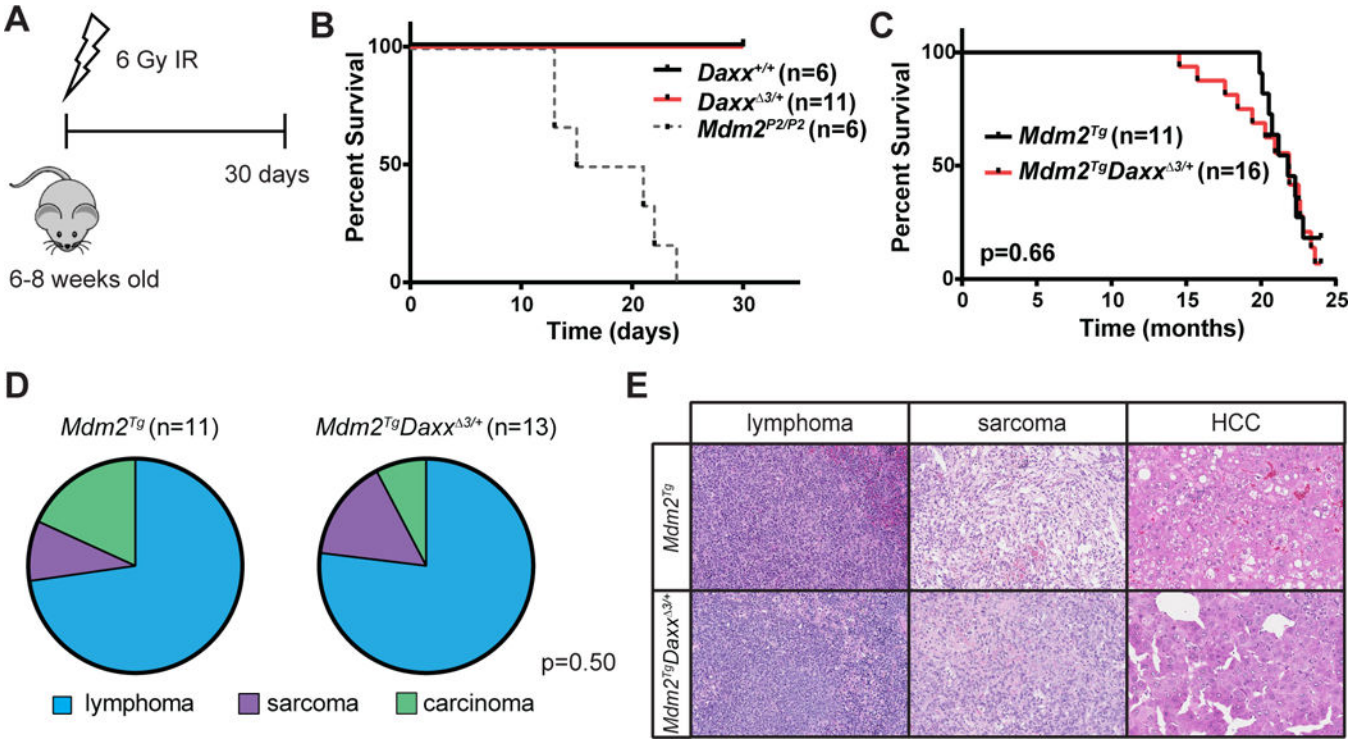

Figure 2: Lack of genetic interaction between Daxx and the p53 pathway *in vivo*.

A) Schematic representation of radiosensitivity experiment. Mice were treated with a single sublethal (6 Gy) dose of ionizing radiation (IR) and monitored for evidence of morbidity due to enhanced radiosensitivity. B) Survival analysis of mice treated with 6 Gy IR. C) Survival analysis of *Mdm2*^{Tg} and *Mdm2*^{Tg}*Daxx*$^{\Delta 3/+}$ mice. D) Tumor spectrum of mice from both genotypes. Tumors that were present in moribund mice are included in this analysis. No significant difference (Chi-squared p=0.50) in the proportions of different tumor types in *Mdm2*^{Tg}*Daxx*$^{\Delta 3/+}$ compared to those expected from *Mdm2*^{Tg} controls. E) Representative histology of tumors from both groups, with lymphomas, sarcomas and hepatocellular carcinomas (HCCs) presented. Images are at 20x magnification.

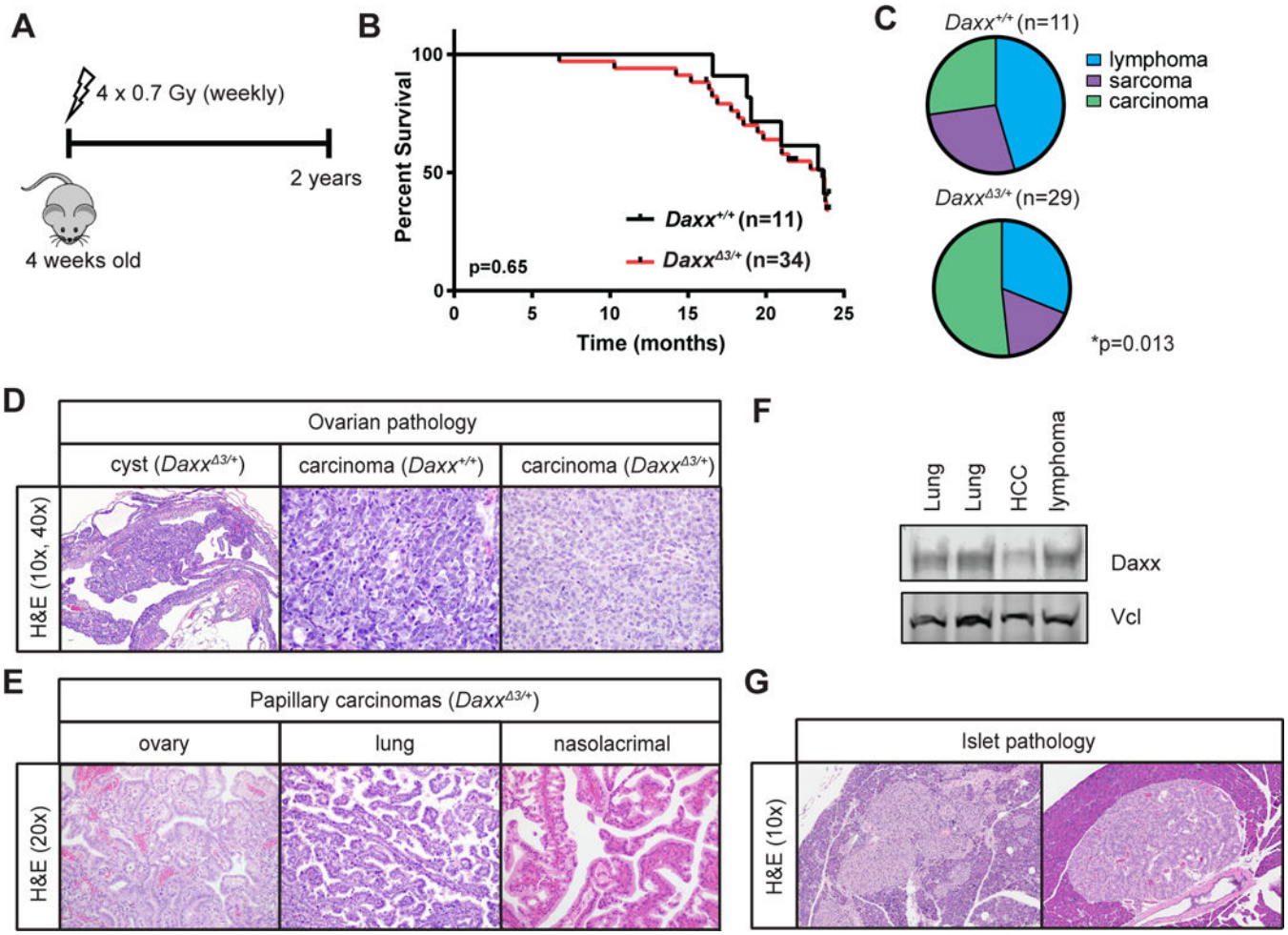

Figure 3: Daxx heterozygosity contributes to carcinoma development in cooperation with low dose ionizing radiation.

A) Schematic representation of experimental procedure. Mice were treated with four weekly doses of ionizing radiation (IR, 4 × 0.7 Gy), starting at 4 weeks of age. Mice were monitored until moribund, or until the 2-year experimental endpoint. B) Survival analysis. C) Tumor spectrum of mice from both genotypes. Chi-squared analysis of the proportions of different tumor types in *Daxx*$^{\Delta 3/+}$ compared to those expected from wild-type controls, *p<0.013. Tumors that were present when mice were moribund or autopsied are included in this analysis. D) Representative H&E sections of identified ovarian pathology from both genotypes. Cysts were identified only in *Daxx*$^{\Delta 3/+}$ mice, and carcinomas in both genotypes. Cyst is at 10x and carcinomas at 40x magnification. E) Representative H&E sections of papillary carcinomas observed in *Daxx*$^{\Delta 3/+}$ mice. Images are at 20x magnification. F) Immunoblot analysis of four *Daxx*$^{\Delta 3/+}$ tumors. HCC, hepatocellular carcinoma; Vcl, vinculin. G) H&E sections of islet pathology identified in *Daxx*$^{\Delta 3/+}$ mice. Images are at 10x magnification.

Table 1:

p53 loss does not rescue *Daxx*-null embryo lethality $Daxx^{\Delta 3/+}p53^{+/-}$ X $Daxx^{\Delta 3/+}$ $p53^{+/-}$

Daxx	*p53*	Expected # (%)	Observed # (%)
+/+	*+/+*	5.2 (6.25)	10 (12.0)
+/+	*+/−*	10.4 (12.5)	17 (20.4)
+/+	*−/−*	5.2 (6.25)	3 (3.6)
Δ3/+	*+/+*	10.4 (12.5)	18 (21.7)
Δ3/+	*+/−*	20.8 (25)	28 (33.7)
Δ3/+	*−/−*	10.4 (12.5)	7 (8.4)
Δ3/Δ3	*+/+*	5.2 (6.25)	0 (0)
Δ3/Δ3	*+/−*	10.4 (12.5)	0 (0)
Δ3/Δ3	*−/−*	5.2 (6.25)	0 (0)
Total		83 (100)	83 (100)

Table 2:

Summary of pathology from moribund *Mdm2*^{Tg} mice

	Mdm2^{Tg}	*Mdm2*^{Tg}*Daxx*$^{\Delta 3/+}$
Mice	**n=9 (%)**	**n=13 (%)**
Cancers	8 (89%)	11 (85%)
Ovarian cyst	0 (0%)	1 (8%)
No pathology	1 (11%)	2 (15%)
Tumors	**n=11 (%)**	**n=13 (%)**
Lymphoma	8 (73%)	10 (77%)
Sarcoma	1 (9%)	2 (15%)
Carcinoma (HCC)	2 (18%)	1 (8%)

Table 3:

Summary of pathology from IR cohort

	Daxx$^{+/+}$	*Daxx*$^{\Delta 3/+}$
Mice	**n=7 (%)**	**n=20 (%)**
Cancers	6 (86%)	18 (90%)
Other pathology	2 (28%)	7 (35%)
ovarian cyst	0	3
islet cell hyperplasia	0	2
myocardial infarction	0	1
infection	2	1
No pathology	1 (14%)	0 (0%)
Tumors	**n=11 (%)**	**n=29 (%)**
Lymphoma/Leukemia	5 (45%)	9 (31%)
Sarcoma	3 (27%)	5 (17%)
Carcinoma	3 (27%)	15 (52%)
Carcinomas	**n=3**	**n=15**
Ovary	1	2
Lung	2	6
Nasolacrimal	0	4
Other	0	3